

## Operational diagrams for MHD instabilities limiting plasma performances in JET D-T Scenarios with ILW

E. Alessi<sup>1</sup>, P. Buratti<sup>2</sup>, E. Giovannozzi<sup>2</sup>, T. O'Gorman<sup>3</sup>, G. Pucella<sup>2</sup>, M. Baruzzo<sup>4</sup>, E. Joffrin<sup>5</sup>,  
S. Nowak<sup>1</sup>, F.G. Rimini<sup>3</sup> and JET Contributors\*

*EUROfusion Consortium, JET, Culham Science Centre, Abingdon, OX14 3DB, UK*

<sup>1</sup>IFP-CNR, via R. Cozzi 53, Milano, Italy; <sup>2</sup>ENEA C. R. Frascati, via E. Fermi 45, Frascati (Roma), Italy; <sup>3</sup>CCFE, Culham Science Centre, Abingdon, United Kingdom; <sup>4</sup>Consorzio RFX, Corso Stati Uniti 4, Padova, Italy; <sup>5</sup>CEA, IRFM, Saint Paul Lez Durance, France

(\*) See the author list of X. Litaudon et al 2017 Nucl. Fusion 57 102001

One of the major aims of nowadays JET experimental campaigns is the execution of D-T experiments with the ILW, ITER-like wall [1-2]. At present, experiments are devoted to develop scenarios capable of sustaining high performances for >5s. Two scenarios are considered for this aim: the Baseline H-mode Scenario, and the Hybrid Scenario.

A statistical survey of the MHD onset conditions for both scenarios is here presented in order to identify the conditions under which Neoclassical Tearing Modes (NTM) are the main causes limiting the plasma performances.

High performances and duration can be limited by the onset of MHD modes or by the influx of high Z impurities in the plasma core [3,4,5]. These two effects have to be disentangled to provide information on the MHD limits of the top performance phase. MHD can foster the accumulation of impurities [4] and, as the present analysis will show, different cases of MHD instabilities at low plasma performances are correlated with plasmas already degraded by Impurity Accumulation (IA).

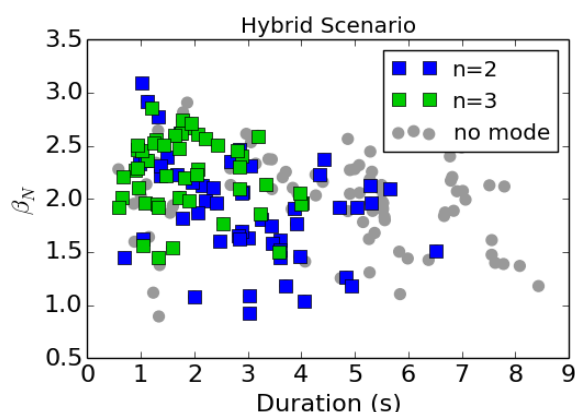
For each scenario, a database has been obtained by collecting the information on MHD instabilities for each pulse. Toroidal numbers (n) and mode amplitudes (in terms of poloidal field oscillations) are estimated by means of the cross-spectral analysis on a toroidal array of Mirnov coils, while the identification of poloidal numbers is obtained by comparison of the mode frequency with the plasma rotation profile and the q profile, as described in [3, 6, 7].

**Hybrid Scenario.** The database includes the phases with high additional heating (NBI>10MW) achieved in ~185 pulses performed during the 2015-2016 JET campaigns. Cross-spectral analysis is sensitive to coherent magnetic fluctuations with amplitude greater than the noise background, however, as pointed out in [3,6,7], not all detections correspond to persistent NTMs with an island width large enough to affect the confinement [6, 9]. Present database is made up of the onset times of n=2,3 instabilities living >~100ms and with an initial width  $W>2.5\text{cm}$ . The island width can be estimated in terms of  $\tilde{B}_\theta/B_T$  (Poloidal magnetic fluctuation normalized to the toroidal magnetic field) by means of

$W = 4 \sqrt{\frac{r_s \cdot R_0}{n \cdot s \cdot B_T} \frac{1}{2} \frac{a_{coil}^{m+1}}{r_s^{m+1}} \tilde{B}_\theta}$  [12], where  $a_{coil}$  is the distance of the coil from plasma axis,  $R_0$  is

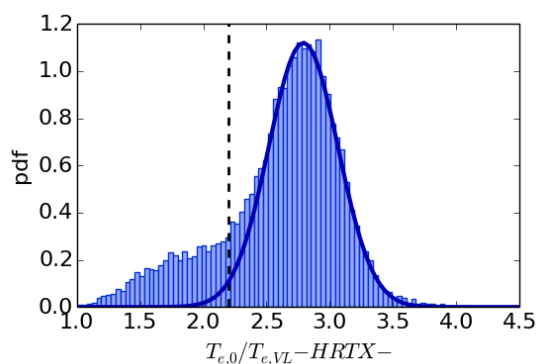
the major radius of plasma axis,  $s$  is the magnetic shear at the resonant surface  $r=r_s$  for  $q=m/n$ . Estimates of typical values for  $s$  and  $r_s$  for  $q=3/2, 4/3$  Islands were calculated using equilibrium reconstruction constrained by Motional Stark Effect (MSE) diagnostics in the database used in [4,7]. This analysis led to pose the following thresholds for detection of  $W>2.5\text{cm}$  islands:  $\tilde{B}_\theta > A_{m/n} \cdot B_T$ , with  $A_{m/n}=1.2 \cdot 10^{-5}, 4 \cdot 10^{-6}$  for  $n=2,3$  respectively.

Figure 1 shows the  $\beta_N$  vs Duration diagram for the Hybrid Scenario.



**Figure 1.** The  $\beta_N$  values at the first time of instability detection (mode onset) during a discharge are shown against the time lag (Duration) with respect to the start of main heating phase. Pulses without  $n=2,3$  instabilities are represented by the  $\beta_N$  at the time of the maximum diamagnetic plasma energy  $W_{MAX}$ , and the duration of the phase  $W>0.8 \cdot W_{MAX}$ , for comparison. Several  $n=2$  and  $3$  modes triggered at low  $\beta_N$  ( $<2.0$ ) are visible in Figure, likely related with core accumulation of impurity.

Core impurity ingress changes the temperature and the current density profiles [8] from peaked to hollow. The estimate of the  $T_e$  peaking ( $T_{e,p} = T_{e,0}/T_{e,vL}$ : the ratio between the central and the volume averaged  $T_e$ ) from High Resolution Thomson Scattering (HRTX) diagnostics has been adopted as a signal to detect the detrimental effect of impurities on electron temperature profile. The probability distribution function (pdf) of  $T_{e,p}$  for Hybrid pulses during the  $\text{NBI}>10\text{MW}$  phase is shown in Figure 2. It looks like a normal distribution centered  $\sim 2.8$ , but with a tail for  $T_{e,p}<2.2$  which is identified as the effect of the IA after comparison pulse by pulse with the radiation level.



**Figure 2.** Statistics of  $T_e$  peaking in Hybrid scenario

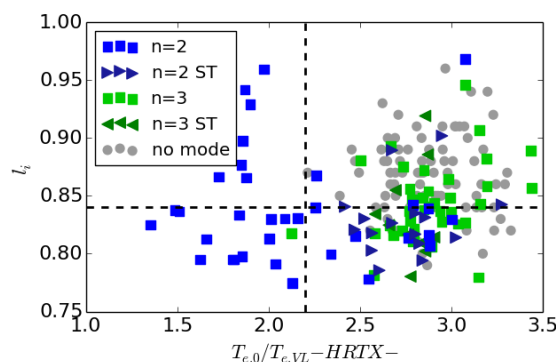


**Figure 3.**  $T_{e,p}$  vs  $l_i$  diagram

A "form factors diagram", i.e.  $T_{e,p}$  vs  $I_i$  at the mode onset and at top performances in pulses without modes, is shown in Figure 3. This diagram suggests the presence of a "stable space" for  $T_{e,p} > 2.2$ ,  $I_i > \sim 0.84$ , less prone to trigger  $n=2$  modes. Modes  $n=2,3$  (blue and green symbols in Figure 3, respectively) are represented with triangles when triggered by Sawtooth crash. ST crashes are a rare cause of mode triggering for low  $T_{e,p}$ , probably due to the absence of the  $q=1$  during IA.

Modes triggered with  $T_{e,p} < 2.2$  (indicated as hollow profile, HP) are shown by diamonds in Figure 4 in the  $\beta_N$  vs  $q_{95}$  plan, they correspond to the majority of the modes triggered at  $\beta_N < 2.0$ .

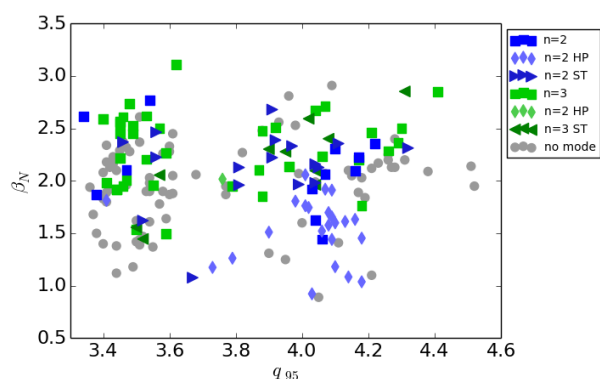


**Figure 4.**  $\beta_N$  vs  $q_{95}$  for Hybrid database. Grey circles represent the values at top performances for pulses without modes. Trigger causes: spontaneous, ST crashes, hollow profile are represented by squares, triangles and diamonds respectively; both for  $n=2,3$  (blue and green colors respectively).

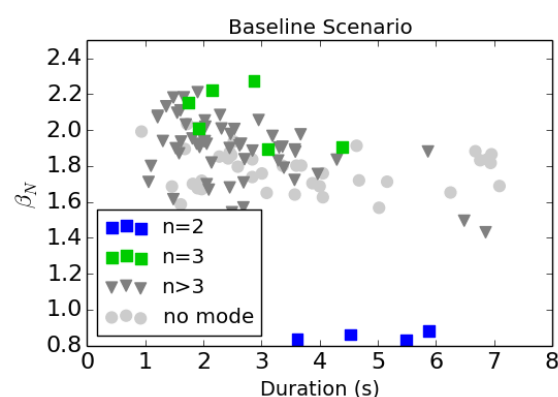


**Figure 5.**  $\beta_N$  vs Duration diagram (see figure 1). Here  $n=4,5$  (grey triangles) are represented together to highlight occurrence of  $n=2,3$  modes (blue and green squares respectively).

**Baseline Scenario.** The database includes the phase of main heating (NBI > 10 MW) for a selected list of  $\sim 90$  pulses with  $q_{95}$  ranging between 2.8-3.3 and  $I_p$  between 2.5-3.5 MA. Some pulses with low performances showed the presence of high- $n$  modes, the present analysis has been extended to modes with  $n$  up to 5 to investigate their effects on plasma performances. A database to estimate Amplitude thresholds for mode detection as done for Hybrid Scenario is still under preparation. In the present work, fixed thresholds in the mode amplitude (poloidal magnetic field) are used -similar to those in [3,4] for  $n=2,3$ - :  $B_{TH,n} = (\sqrt{10})^{1-n}$  Gauss for  $n=2,3,4,5$ . In Figure 5 the  $\beta_N$  vs duration diagram is shown for  $n=2,3$  separately and  $n=4,5$  together. Few cases of long living  $n=2$  are detected at low  $\beta_N$ , also these cases result as due to IA.

An estimate of the effects of the modes on confinement is given in Figure 6 as  $\Delta\beta_N = \beta_{N,0.75} - \beta_{N,onset}$  the change on  $\beta_N$  after 0.75s (or when the mode disappears if shorter) from the mode onset. Negative  $\Delta\beta_N$  are related with confinement degradation. High  $n$  modes (4,5) have  $\Delta\beta_N < 0$  only in certain cases (in particular, if triggered with  $\beta_N$  within 1.8-2.1), while  $n=2,3$

modes are always correlated with  $\Delta\beta_N < 0$ . The present statistical approach does not show a clear detrimental role of modes with  $n=4,5$ . This may be due to their onset in the early stage of the main heating phase, or to the correlation with other kinds of events [4].  $n=2$  modes are all triggered after an IA, and then only  $n=3$  modes appear limiting the performances in the present Baseline database. Onsets of  $n=3$  draw a linear trend in the  $\beta_N$ - $q_{95}$  plane, similar to a beta limit, in Figure 7, and indicating that higher  $q_{95}$  may have access to higher  $\beta_N$ . It is worth noticing that there is no difference between the  $\beta_N$  onset values for  $n=3$  cases triggered by sawteeth and the spontaneous one.

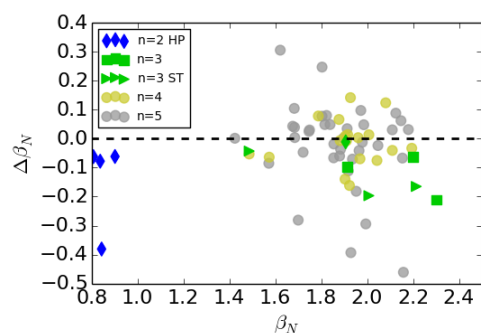


**Figure 6.** Confinement loss  $\Delta\beta_N$  vs  $\beta_N$

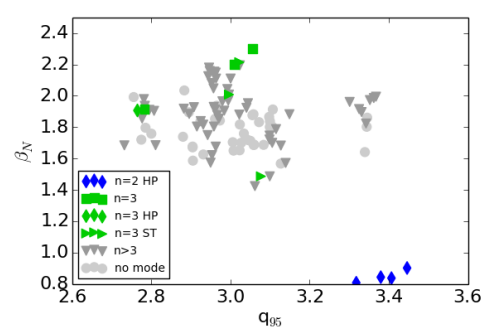


**Figure 7.**  $\beta_N$  vs  $q_{95}$  diagram

**Conclusions.** Present statistical overview on the two main scenarios devoted to DT experiments at JET shows a greater MHD instability of the Hybrid scenario, as in previous campaigns [10]. This is due to the different range of poloidal beta  $\beta_p$  explored by the two scenarios:  $\sim 0.6$ - $0.8$  for Baseline; and  $\sim 0.8$ - $1.2$  for Hybrid. Different MHD instabilities can be triggered at lower performances than expected ( $\beta_N < \sim 1$ ) as a consequence of the IA, these cases are discriminated by introducing the variable  $T_{e,p}$ . The nature of such MHD is to be further analysed by modeling (see [11]). Values of  $\beta_N$ ,  $\beta_p$ ,  $T_{e,p}$  are linearly correlated one each other, and a linear correlation is also expected between  $\beta_p$  and  $I_p$ . However, a sharper edge between a stable and an unstable region for Hybrid ( $n=2$ ) appears in the "form factors" diagram of Figure 3.  $n=3$  modes look like the most dangerous in Baseline scenario, and their  $\beta_N$  values at mode onset show a linear relationship with  $q_{95}$  (see Figure 7).

**Acknowledgements** This work has been carried out within the framework of the EUROfusion Consortium and has received funding from the Euratom research and training programme 2014-2018 under grant agreement No.633053. The views and opinions expressed herein do not necessarily reflect those of the European Commission.

#### **References:**

- [1] X. Litaudon et al 2017 *Nucl. Fusion* **57** 102001; [2] L. Horton et al 2016 *Fusion Eng. Des.* **109–11** 925; [3] P. Buratti et al 2015 *42nd EPS Conf. on Plasma Physics (Lisbon)* P2.115; [4] T. Hender et al 2016 *Nucl. Fusion* **56** 066002; [5] I Nunes 2016 *Plasma Phys. Control. Fusion* **58** 014034; [6] P. Buratti et al 2014 *41st EPS Conf. on Plasma Physics (Berlin)* P1.104; [7] P. Buratti et al 2016 *Nucl. Fusion* **56** 076004; [8] P. de Vries et al 2014 *Physics of Plasmas* **21** 056101; [9] T.C. Hender et al 2007 *Nucl. Fusion* **47** S128; [10] D. Frigione et al 2015 *42nd EPS Conf. on Plasma Physics (Lisbon)* P2.116; [11] G. Pucella et al. submitted at the 2<sup>nd</sup> Asia-Pacific Conference on Plasma Physics, Japan, 12/11/2018; [12] R. Fitzpatrick 1995 *Phys. Plasmas* **2** 825